Numerical Solution of the Coupled Nernst−Planck and Poisson Equations for Liquid Junction and Ion Selective Membrane Potentials

Tomasz Sokalski,[†,‡] Peter Lingenfelter,[†] and Andrzej Lewenstam*[,†,§]

Process Chemistry Group, c/o Centre for Process Analytical Chemistry and Sensor Technology (ProSens), Åbo Akademi University, Biskopsgatan 8, FIN-20500 Åbo/Turku, Finland, Department of Chemistry, University of Warsaw, 02093 Warsaw, Poland, and Faculty of Material Science and Ceramics, University of Mining and Metallurgy, 30059 Cracow, Poland

Received: June 28, 2002; In Final Form: November 27, 2002

A new numerical model is presented for analyzing the propagation of ionic concentrations and electrical potential in space and time in the liquid junction and in the solution/ion-exchanging membrane system. In this model, diffusion and migration according to the Nernst−Planck (NP) flux equation govern the transport of ions, and the electrical interaction of the species is described by the Poisson (P) equation. These two equations and the continuity equation form a system of partial nonlinear differential equations that is solved numerically. This yields the Nernst−Planck−Poisson (NPP) model that we exploit in this paper. Notably, as a result of the physicochemical properties of the system, which are clearly defined in this paper, both the contact/boundary potential and the diffusion potential contribute to the overall membrane potential. Previously, only the boundary potential at steady state was considered due to some arbitrary and clearly untested assumptions. By accessing space and time domains, it is shown that interpreting the electrical potential of ion-exchanging membranes exclusively in terms of boundary potential at steady state is incorrect. The NPP model is general and applies to ions of any charge in space and time domains. It is shown for the first time that the paradigmatic equations for every open circuit measurement, such as the Henderson liquid junction equation or the Nikolskii−Eisenman equation, are special cases of the NPP model. The NPP model is not only more rigorous but also more complete than previous models, and it is proposed to be a more appropriate and updated platform for dealing with the theory of ion selective membrane electrodes for analytical applications.

1. Introduction

Charge separation and transport of ions in two phase systems (e.g., liquid−liquid and/or solid−liquid) and the resulting electrical potential difference at the interface (membrane) are a prerequisite for open circuit electroanalytical methods, e.g., potentiometry with ion selective membrane electrodes (ISEs). The same membrane processes are of vital importance in cell biology as well, since they support homeostasis of living organisms. Although both membrane electroanalytical chemistry and membrane biophysics share a common interest in membranes and should therefore share common principles in theoretical modeling, the present modeling approaches in these two fields are distinctly different.

The prevalent approach in ISE modeling is to relate the processes of ion exchange and membrane transport to the operationally defined electrical potential of the ion selective electrode or even—as in the case of pH standardization (BSI)—to a fully operationally defined procedure involving primary and secondary standards. This restricts the theoretical modeling to interpretations based on, and biased toward, empirical postulates in the form of empirical equations.[1,2] A general equation postulate of this type, accepted widely in the ISE field, is the Nikolskii−Eisenman (NE) equation[3,4] (see eq 10 below).

This practice is in stark contrast to the theoretical routines in membrane science or biophysics, in which membranes and membrane channels are regularly modeled with the Nernst−Planck−Poisson (NPP) system of partial differential equations.[5−10] There are two reasons for this situation. One is that analytical chemistry, which includes the field of ISEs, is an applied science;[11] the other is the substantial formal difficulty in using the NPP theory. The NPP model is a system of coupled nonlinear partial differential equations, which cannot be solved analytically. This difficulty was overcome with the advent of numerical methods and computer processors fast enough to use them. Explicit (nonpredictive) and implicit (predictive) numerical methods for solving these "unsolvable" equations or systems of equations were first proposed in the 1950s alongside the arrival of digital computers. The first publication to herald the application of these methods to the NPP system of equations was the historical work by Cohen and Cooley,[12] which provided the first time-dependent numerical solution of the NPP equation system. Hafemann[13] then went on to simulate liquid junction potentials and ion concentration profiles over the liquid junction as a function of time. MacGillivray, in his classic papers, analyzed the application of the Nernst−Planck (NP) equations.[14,15] These works made possible the first numerical solution of the NPP equation system relevant to then current ISE research by Brumleve and Buck,[16] who solved the NPP system via a fully implicit iterative Newton−Raphson method coupled to Gaussian elimination in FORTRAN. This fundamental work was later taken up and continued by several groups, including

* To whom correspondence should be addressed. Tel: +358 2 215 4418. Fax: +358 2 215 4479. E-mail: Andrzej.Lewenstam@abo.fi.
† Åbo Akademi University.
‡ University of Warsaw.
§ University of Mining and Metallurgy.

10.1021/jp026406a CCC: $25.00
Published on Web 02/21/2003

significant contributions by Mafé, Manzanares, and Kontturi.[17−23] Additional numerical methods, such as fast implicit finite difference,[24] finite element,[25] and network simulation[26] have also been proposed but for interpreting other electrochemical problems.

Brumleve and Buck's model[16] supplied many elements worth retaining for further research. The aforementioned method of solving the system via Newton−Raphson iteration coupled to Gaussian elimination was found to be more than adequate. Space and time grids were also formulated. However, their approach imposed a need for reformulation of the code on a case-by-case basis and did not allow for flexible redefinition of the problem. Moreover, undoubtedly because of time restrictions imposed by computing power (or the lack thereof), Brumleve and Buck did not provide time−potential or time−concentration profiles, opting for only steady state space−concentration distributions. To the extent that the authors can be certain, in the field of ISEs, only steady state spatial−concentration distributions have been generated, whereas the even more essential space and time profiles have not. This research attempts to correct this omission by using nearly the same strategy but written in C++. C++ was chosen in order to employ ready-made numerical method classes, which greatly simplifies what would otherwise be a daunting task.[27] Herein, a unique quality of C++ is deliberately exploited, i.e., the possibility of cumulative enlargement of libraries, which allows the application of prewritten classes to a new problem without the laborious work of changing the program.

This paper presents the simulated concentration and potential profiles for liquid−liquid and liquid−membrane systems in the explicit space and time domains. It provides new information regarding several issues that have recently been introduced elsewhere.[28] It gives detailed insight into the formation of ion sensitive membrane electrical potential as a function of space and time, thus providing a tool for inspecting dynamic properties of ion sensitive membranes. Long-debated problems concerning the mechanisms of membrane potential, such as the contribution of diffusion potential to the overall membrane potential, are discussed.

Finally, the paradigmatic equations in potentiometry—the Henderson and NE equations—are shown to be special cases of the NPP model. This naturally prompts questioning the soundness of widespread use of these equations, if a more accurate solution exists.

2. Theoretical

2.1. Physicochemical Model. To discuss membrane potential, a symmetrical system is considered as follows: solution (left)/membrane/solution (right). The membrane in contact with the aqueous bathing solutions is assumed to be flat, isotropic, and of thickness d meters. The membrane contains mobile and/or fixed R^- sites confined to the membrane, and ions of any charge are extracted to/from the bathing solutions. No association between extracted ions and R^- sites is considered. Convection and/or solvent flow are ignored.

For the analysis of liquid junction potential, a symmetrical system containing "contact zone"[20,29] is considered as follows: solution (left)/contact zone/solution (right). The contact zone in this system is assumed to have no effect on the solution in it.

All activity coefficients are assumed to be one, and the diffusion coefficients are constant for a given ion (i.e., $D_i(c,x,t)$ = constant). Ion extraction is described by appropriate first-order rate constants.

The NPP model presented above is idealized in many respects. The model adopted here uses an idealized approach known as dilute solution.[16] For simplicity, the activity coefficients are considered to be unity even for high concentrations of multivalent salts. It is also assumed that water concentration, and in consequence the dielectric permittivity and the effective diffusion coefficients, are constant throughout the membrane. This may not be strictly valid. The problem of uneven water distribution, especially in poly(vinyl chloride) (PVC)−membrane surface regions, is discussed by some authors.[30−32] This important issue is not discussed within the framework of the present version of the NPP model. However, this approach is sufficient to fulfill the goal of this paper, which only focuses on the problem of concentration and electrostatic potential profiles in space and time, throughout the liquid junction and/or membrane.

2.2. Mathematical Model. Ion flux in space (x) and time (t) is described by the NP equation,[33−36] which in one dimension reads

$$f_i(x,t) = -D_i\left[\frac{\partial c_i(x,t)}{\partial x} - z_i c_i(x,t)\left(\frac{F}{R \cdot T}\right)E(x,t)\right] \qquad (1)$$

where $f_i(x,t)$ is the flux of the ith ion, $c_i(x,t)$ is the concentration of the ith ion, D_i is the diffusion coefficient of the ith ion, z_i is the charge of the ith ion, $E(x,t)$ is the electrical field, and R, T, and F have their usual meanings.

To solve eq 1, two additional equations are needed to relate the flux, $f_i(x,t)$, $c_i(x,t)$, and $E(x,t)$. One obvious choice is the law of mass conservation (also referred to as the continuity equation):

$$\frac{\partial c_i(x,t)}{\partial t} = -\frac{\partial f_i(x,t)}{\partial x} \qquad (2)$$

and the second is the Poisson equation:

$$\frac{\partial E(x,t)}{\partial x} = \frac{\rho(x,t)}{\epsilon};\ \rho(x,t) = F \cdot \sum_i z_i \cdot c_i(x,t) \qquad (3)$$

or the totally equivalent and, in this case more convenient, density current ($I(x,t)$) equation:[12]

$$I(x,t) = F \cdot \sum_i z_i \cdot f_i(x,t) + \epsilon \cdot \frac{\partial E(x,t)}{\partial t} \qquad (4)$$

where $\rho(x,t)$ is the charge density and ϵ is the dielectric permittivity. This set of equations (1, 2, and 4) is solved for any number of ions and any ionic charge for $I(x,t) = 0$.

In all calculations, the following boundary conditions were used

$$f_{i0}(t) = \vec{k}_i \cdot c_{i,\mathrm{bL}} - \overleftarrow{k}_i \cdot c_{i0}(t) \qquad (5a)$$

$$f_{id}(t) = -\vec{k}_i \cdot c_{i,\mathrm{bR}} + \overleftarrow{k}_i \cdot c_{id}(t) \qquad (5b)$$

where f_{i0}, f_{id}, c_{i0}, c_{id} are the fluxes and concentrations at $x = 0$ and $x = d$, $\vec{k}$ and $\overleftarrow{k}$ are the forward and backward rate constants, and $c_{i,\mathrm{bL}}$ and $c_{i,\mathrm{bR}}$ are the concentrations in the bathing solutions of the left and right side, respectively.

For a liquid junction, $\vec{k}$ *and* $\overleftarrow{k}$ from eqs 5a,b have the physical meaning of fluxes at $x = 0$ and $x = d$, respectively, at unit ion concentration. In this case, "nearly infinite" constants, i.e., 10^4 cm/s, are used.

2.3. Numerical Model. A totally implicit finite difference method was utilized. First, eqs 1, 2, and 4 are discretized in space and time. The resulting system of difference equations is solved by the Newton−Raphson method, which can be expressed as follows:

$$\mathbf{J}(\mathbf{x}^{(i)})\,\Delta\mathbf{x}^{(i+1)} = -\mathbf{F}(\mathbf{x}^{(i)}) \qquad (6)$$

where $\mathbf{J} \equiv \nabla\mathbf{F}$, the Jacobian of $\mathbf{F}$.

Iterations are continued until the convergence criterion is reached. For details, see appendix A in the Supporting Information.

The program code is written in the C++ programming environment, using numerical specialized libraries for solving partial difference equations provided by DiffPack (Numerical Objects AS, Norway). The object-oriented nature of the C++ language and modularity of the DiffPack libraries make the code highly reusable. The simulations were executed on a 1.5 GHz PIV computer with 512 Mb RAM. The efficiency of the code reduces the computation time to around 10 s for 1000 spatial grid points and 25 temporal grid points.

Because of all of the assumptions of a physicochemical, mathematical, numerical, or computational nature, the NPP model—like every model[2]—is approximate. Nevertheless, even at this level of approximation, many systems of significance to both ISE research and membrane science in general can be analyzed. More details concerning the mathematical model can be found in appendix A of the Supporting Information.

3. Results and Discussion

The model described in the previous section was used to simulate several commonly discussed examples. The problem of junction potential between two liquids—a subject of interest for well over a century—will be discussed first, followed by interpretation of the response of ISEs. Finally, comparisons are drawn between the NPP model and the other models used for interpreting the electrochemical properties of ion sensitive membranes.

3.1. Critical Remarks on the NPP Approach. Before commencing on a detailed presentation of the numerical results, some aspects of the NP, continuity, and Poisson equations, which make up the "backbone" of the NPP model, require closer examination.

NP Equation. This equation and its application can be criticized for several reasons, as Buck pointed out in his excellent review.[37] The main reasons are the "macroscopic, smooth nature of the model used in its derivation" and the omission of "cross terms". Despite these major objections, he remarks upon its "surprising usefulness and wide applicability."

Incidentally, these objections seem to be of little or no importance in the case of ion selective membranes, since such membranes are relatively thick (with respect to Debye length) and homogeneous. Furthermore, in the case of plastic membranes such as those discussed here, the components' concentrations are of the order of 10^{-3} M (dilute), so cross terms may be ignored. The low ionic strength in the membrane also warrants the use of concentrations instead of activities. Hence, the NP equation seems to be tailor-made for the description of ion selective membranes.

For the boundary conditions, first-order kinetics is used. It is true that this may be considered crude. Introducing higher order kinetics is feasible, but first-order kinetics is sufficient for this research, where the main goal was to apply the NPP model.

Continuity Equation. It is an equivalent term for the law of mass conservation, which is undoubtedly one of the main and unchallenged laws of physics. It cannot be reasonably disputed. It provides the basic (and only) connection between space and time changes of physical quantities (concentration and electric field in the case in this paper).

In most important models related to the liquid junction and/or membranes, this equation is purposely omitted, by assuming a steady state, i.e., $dc/dt = 0$, thus avoiding the technical difficulties stemming from solving time-dependent equations. Various and often ingenious methods have been applied to achieve algebraic resolutions using this assumption, and these solutions themselves encompass a large share of scientific history.[29,33−36,38−51] Unfortunately, this technical difficulty is often masked by the (mostly verbal) declaration of the lack of interest in transient processes. The great advantage of the NPP model is its ability to describe accurately the time evolution of membrane potential. This is naturally needed for ISEs as it may take a long time (minutes or even hours) for ISE membranes to reach steady state, as has been shown[16,28] and will be discussed later.

Poisson Equation. One of the most commonly used assumptions, which considerably simplifies calculations, is the electroneutrality condition (ELC) within the membrane. However, if not clearly understood, its implementation can result in profound confusion. For more details, see appendix B in the Supporting Information. It should be stressed that the ELC is not equivalent to assuming $\rho = 0$ but rather to approximating $c_1 \cong c_2$.[52,53]

It has been convincingly demonstrated[13,20] that the ELC is justified in certain cases, for instance for steady state and for distances greater than one Debye length in liquid junctions. These conditions are more likely to be fulfilled for a direct liquid junction where a steady state may develop as quickly as 10^{-9} seconds. For ISE liquid membranes, however, departure from the ELC is especially pronounced in proximity to the membrane−water interface, even at steady state.

In light of this, it is naturally preferable to use the Poisson equation whenever possible, as it is generally valid. One should refrain from using the ELC, unless absolutely necessary, and only on a case-to-case basis.

3.2. Junction Potential. *3.2.1. Conventional Modeling Patterns.* The formulation of the problem and the first mathematical modeling of a liquid junction potential is credited to Planck.[35,36] He considered the so-called "constrained diffusion" boundary, where solutions of 1:1 electrolytes are connected by means of a porous plug.[29] The diffusion through the plug was assumed to be at steady state, at which point one may assume that electroneutrality holds. With these assumptions, eq 1 could be rewritten and integrated. A similar approach was later used by Henderson[40,41] who assumed a "mixture boundary" between two solutions containing electrolytes with linear profiles for all ions. Since then, other scientists have regularly employed these two models. In the 1970s, Morf[54] reworked the problem in an elegant manner. This author presented a less circuitous derivation of the Planck problem while retaining all of the Planck model's idealized assumptions regarding the diffusion layer.

3.2.2. Numerical Results by NPP. To test the NPP model against these historically important results, the junction potentials formed over a "watery contact zone" were studied. A watery contact zone may be described as a barrier separating the two bathing solutions possessing the same physical characteristics as water. In this manner, the steady state values could be compared at infinite time obtained by the NPP equation system with the published values according to the Planck and Henderson

TABLE 1: Liquid Junction Potentials for Different Sample Solutions and KCl Bridge Electrolytes at 25 °C[a]

	sample activity (M)	liquid junction potential (mV) for a salt bridge containing the following concentrations of KCl (M)								
		3.5			1.0			0.1		
		H	P	NPP	H	P	NPP	H	P	NPP
KCl	1	−0.2	−0.2	−0.2	0.0	0.0	0.0	0.4	0.4	0.4
	0.1	−0.6	−0.6	−0.6	−0.4	−0.4	−0.4	0.0	0.0	0.0
	0.01	−1.0	−1.0	−0.9	−0.8	−0.8	−0.7	−0.4	−0.4	−0.4
	0.001	−1.4	−1.4	−0.9	−1.2	−1.2	−0.8	−0.8	−0.8	−0.7
NaCl	1	1.9	1.9	1.9	4.4	4.4	4.4	12.4	12.4	12.4
	0.1	−0.2	−0.2	−0.2	0.7	0.7	0.6	4.4	4.4	4.4
	0.01	−1.0	−1.0	−0.8	−0.6	−0.6	−0.6	0.7	0.7	0.6
	0.001	−1.4	−1.4	−1.4	−1.2	−1.2	−0.8	−0.6	−0.6	−0.6
$CaCl_2$	0.5	3.7	*a*	3.5	8.0		7.9	21.3		22.4
	0.05	0.2		0.2	1.6		1.5	8.0		7.9
	0.005	−0.9		−0.9	−0.5		−0.4	1.6		1.5
	0.0005	−1.4		−1.4	−1.2		−1.1	−0.5		−0.4
HCl	1	−15.1	−16.2	−16.2	−26.8	−26.8	−26.8	−57.5	−52.8	−52.8
	0.1	−4.2	−4.9	−4.9	−8.6	−9.7	−9.6	−26.8	−26.8	−26.8
	0.01	−1.5	−1.8	−1.5	−2.4	−2.8	−2.3	−8.6	−9.7	−9.6
	0.001	−1.3	−1.5	−1.0	−1.3	−1.5	−1.0	−2.4	−2.8	−2.3
NaX[c]	1	−6.9	−4.9	−5.8	−14.5	−13.6	−13.4	−44.6	−52.9	−50.6
	0.1	−2.0	−0.8	−1.6	−3.7	−2.0	−3.0	−14.5	−13.6	−13.5
	0.01	−1.4	−0.4	−1.2	−1.5	−0.5	−1.2	−3.7	−2.0	−3.0
	0.001	−1.6	−0.4	−1.4	−1.5	−0.4	−1.3	−1.5	−0.5	−1.3

[a] Values calculated according to the Henderson (H), Planck (P), and NPP methods. [b] For systems in which the ions are of different valences, the NP equation by itself is not valid. The extended theory of Schlögl must be utilized to calculate the potential. [c] X^- is a large, immobile "protein" for which the diffusion coefficient is nearly 0.

TABLE 2: Time Necessary to Reach Steady State Potential as a Function of Anion Mobility

X^- diffusion coefficient (cm^2/s)	time necessary to reach steady state potential
10^{-7}	80 s
10^{-8}	40 min
$\rightarrow 0$	$\rightarrow$22 h

equations (see Table 1).[50] The results are nearly identical. As pointed out earlier, Hafemann showed with his model that steady state liquid junction potentials can be reached after times of the order of 10^{-9} s for direct contact NaCl/NaCl or NaCl/KCl.[13,20,52] Our results confirm that junction potentials for the direct contact NaCl/NaCl or NaCl/KCl systems studied by Hafemann do in fact reach steady state after times of the same order of magnitude. The situation changes considerably (by several orders of magnitude) if instead of direct contact a watery contact zone is used. Figure 1 shows the potential over this type of liquid junction as a function of contact zone thickness and time. The times to reach steady state with a watery contact zone can be measured in seconds rather than nanoseconds even for the infinite rate constants used.

Another factor that influences the potential transient is the mobility of the ions within the diffusion "boundary". Table 2 presents the times needed to reach steady state for different mobilities of monovalent anion X^-. The diffusion coefficient for X^- was varied from 10^{-7} to $\rightarrow 0$ cm^2/s. It was found that even for the "fastest" X^- ($D_X = 10^{-7}$ cm^2/s), the time needed to reach steady state was much higher than in the aforementioned systems for which the anion mobility was 2×10^{-5} cm^2/s.

There is no immediate practical application of the NPP method in the case of liquid junction. However, one may anticipate that this method will be a good tool for analyzing transients on the salt bridge (contact zone) in reference electrodes, which may be a source of error in certain practical situations. For instance, the NPP method could be used to interpret a sluggish response of the reference electrodes with a constrained liquid junction in clinical analyzers, a potential source of analytical error.[55−57] The reference electrode system has thus far been interpreted almost exclusively by the Henderson equation,[58] while the NPP would allow consideration of the finite rate constants and multilayer composition of the bridge (contact zone) with varying ion mobilities and the resulting overall reference electrode potential response.

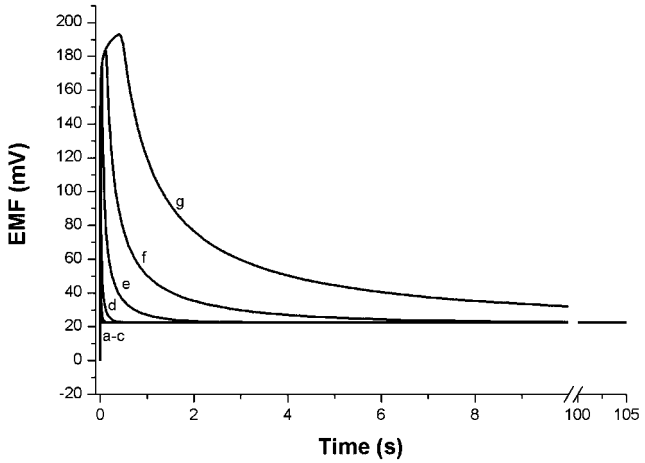

Figure 1. Liquid junction potential as a function of time for $CaCl_2$ solutions. System composition: 0.1 M KCl/0.5 M $CaCl_2$. Diffusion coefficient values were 0.798×10^{-5}, 1.98×10^{-5}, and 2.01×10^{-5} cm^2/s for Ca^{2+}, K^+, and Cl^-, respectively. Forward and backward rate constants of 10^4 cm/s were used for all ions. Contact zone thicknesses were (a) 20, (b) 50, (c) 100, (d) 200, (e) 500, (f) 1000, and (g) 2000 μm.

3.3. ISEs. Before the numerical results of the NPP model for ISEs are presented and in order to create a foundation for presentation, the reasoning behind the traditional modeling of ISEs is reviewed.

3.3.1. Conventional Modeling Patterns. The first ISE, a glass electrode, was invented in 1909.[50] The first theory of glass electrode potential was developed by Dole[38] and later reformulated by Nikolskii.[42] They both took advantage of Guggenheim's[60,61] electrochemical potential concept and derived the equation for the electrical potential at the boundary glass/

solution, the latter containing hydrogen and sodium ions. Nikolskii provided the equation in the form below, whose impact lasts up to today:

$$E = E_B = E^0 + \frac{R \cdot T}{F} \ln\left(\frac{a_{H^+}}{N_{H^+}}\right) = E^0 + \frac{R \cdot T}{F} \ln\left(\frac{a_{H^+} + K \cdot a_{Na^+}}{N_{H^+} + N_{Na^+}}\right) = E^{0'} + \frac{R \cdot T}{F} \ln(a_{H^+} + K \cdot a_{Na^+}) \quad (7)$$

where E is electrode potential, E_B is a boundary potential, E^0 and $E^{0'}$ are constants, a_{H^+} and a_{Na^+} are the activities of hydrogen (main) and sodium (interfering) ions in the solution, K is the equilibrium constant for the ion exchange reaction (bar means the ions are in the membrane phase):

$$\overline{H^+} + Na^+ \rightleftarrows \overline{Na^+} + H^+ \quad (8)$$

where N_{H^+} and N_{Na^+} are the concentrations of the ions in the glass and where $N_{H^+} + N_{Na^+} =$ constant.

Nikolskii consciously disregarded diffusion potential but was of the opinion that "further development of the theory seems to be necessary, and some concepts of the generalized theory should be taken into account in the solution of questions connected with diffusion potentials".[47]

In the 1960s, both Nikolskii and his group[62,63] and Eisenman and co-workers[64−66] independently expressed the overall membrane potential as the sum of the boundary and diffusion potentials under steady state. For the case corresponding to eq 7, the equation obtained by Eisenman is

$$E = E_B + E_D = E^{0'} + \frac{R \cdot T}{F} \ln\left(\frac{a_{H^+}}{N_{H^+}}\right) + \frac{R \cdot T}{F} \ln\left(N_{H^+} + \frac{u_{Na^+}}{u_{H^+}} N_{Na^+}\right) = E^{0'} + \frac{R \cdot T}{F} \ln\left(\frac{a_{H^+} + K \cdot a_{Na^+}}{N_{H^+} + N_{Na^+}}\right)\left(N_{H^+} + \frac{u_{Na^+}}{u_{H^+}} N_{Na^+}\right) = E^{0'} + \frac{R \cdot T}{F} \ln\left(a_{H^+} + \frac{u_{Na^+}}{u_{H^+}} K \cdot a_{Na^+}\right) \quad (9)$$

where E_D is the diffusion potential in the membrane and u_{Na^+} and u_{H^+} are ion mobilities for Na^+ and H^+, respectively.

For $u_{Na^+} = u_{H^+}$, the Eisenman eq 9 reduces to the Nikolskii eq 7, while for $K = 1$, it transforms into a form of a well-known equation in membrane biology known as the constant field Goldman−Hodgkin−Katz equation.[67,68] These equations form the basis of conventional ion selective membrane theory, distinguished by a steady state approach and an arbitrary split of the membrane potential into boundary and diffusion terms.

The emphasis on practical applications of ISEs and on the simplicity of the equation to be used as a working tool later resulted in the decision of the IUPAC to merge the aforementioned eqs 7 and 9 and postulate a general equation for all ISEs, covering all charges of ions, known today as the NE equation:[3,4]

$$E = E^0 + \frac{R \cdot T}{z_M \cdot F} \ln(a_M + \sum K_{M,N}^{pot} a_N^{z_M/z_N}) \quad (10)$$

where a_M is the activity of a main (or primary) ion, a_N is the activity of an interfering ion, z_M and z_N are their respective charges, and $K_{M,N}^{pot}$ is the selectivity coefficient.

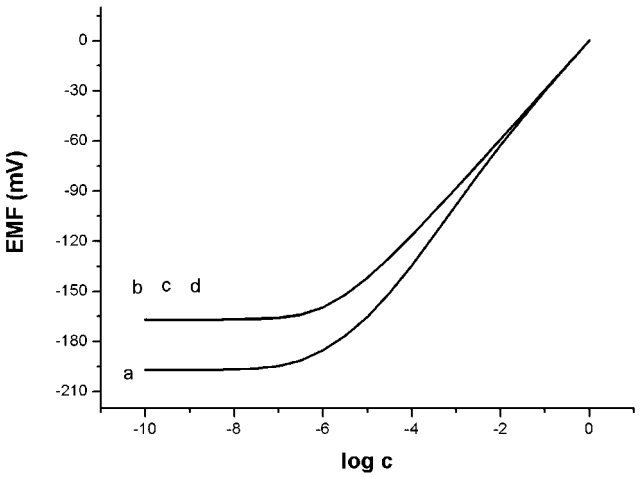

Figure 2. Calibration curves in the presence of primary ($[M^{2+}] = (10^{-10}$ to 10^{-1} M)) and interfering ($[N^+] = 0.15$ M) ions calculated according to (a) NPP model (71 points), (b) NPP model (501 points), (c) NPP model (1001 points). For a−c: $D_M = D_N = D_R = 1.0 \times 10^{-7}$ cm^2/s, $\vec{k}_N = 4.472 \times 10^{-5}$, $\vec{k}_N = \vec{k}_M = \vec{k}_M = 10^{-1}$cm/s ($k_M/k_N = 4.472 \times 10^{-4}$) and (d) Morf model,[50] $K_{M,N} = 10^{-4}$.

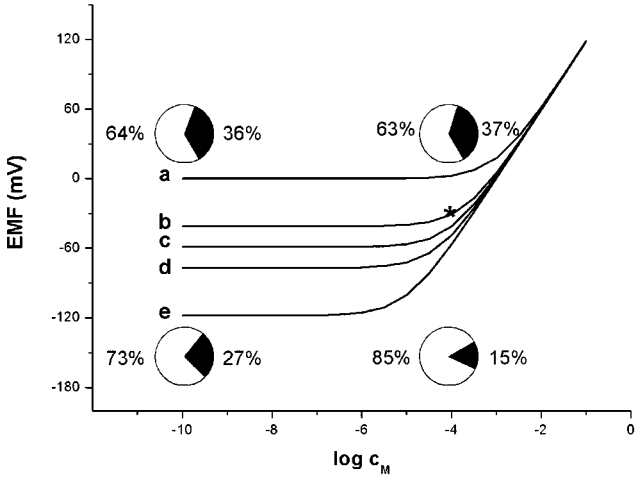

Figure 3. Calibration curves in the presence of primary ($[M^+] = (10^{-10}$ to 10^{-1} M)) and interfering ($[N^+] = 10^{-3}$ M) ions calculated according to the NPP model: (a) $D_M = D_R = 1.0 \times 10^{-7}$, $D_N = 1.0 \times 10^{-6}$ cm^2/s ($D_M/D_N = 0.1$); (b) $D_M = D_R = 1.0 \times 10^{-7}$, $D_N = 2.0 \times 10^{-7}$ cm^2/s ($D_M/D_N = 0.5$); (c) $D_M = D_N = D_R = 1.0 \times 10^{-7}$cm^2/s ($D_M/D_N = 1$); (d) $D_M = 2.0 \times 10^{-7}$, $D_N = D_R = 1.0 \times 10^{-7}$ cm^2/s ($D_M/D_N = 2$); (e) $D_M = 1.0 \times 10^{-6}$, $D_N = D_R = 1.0 \times 10^{-7}$ cm^2/s ($D_M/D_N = 10$), $\vec{k}_M = \vec{k}_M = 10^{-1}$, $\vec{k}_N = 10^{-2}$, $\vec{k}_N = 10^{-1}$, $\vec{k}_X = X = 0$, $k_N/k_M = 0.1$. Pie charts express contributions of boundary potential (white) and inner membrane potential (black) for the outermost calibration curves ($D_M/D_N = 0.1$ or 10) at $[M^+] = 10^{-4}$ and $[M^+] = 10^{-10}$ M.

Although this equation is sufficient for practically oriented analytical chemists, it is misleading if it is the starting point for theorizing. In the common theoretical scheme used to derive the NE equation, certain assumptions are made to allow for calculation; namely, (i) the potential at steady state only is considered, and hence, the potential in the NE equation is time-independent; (ii) the arbitrary split into a boundary and diffusion potential is used and electroneutrality or quasielectroneutrality is assumed.[38,42−44,54,57,65,66,69−77] Additionally, (iii) as a rule, the diffusion potential is purposely ignored, assumed to be negligibly small or constant, and only the boundary potential is considered.[78−82] This latter assumption contradicts recent findings demonstrating drastic improvements in the detection limit

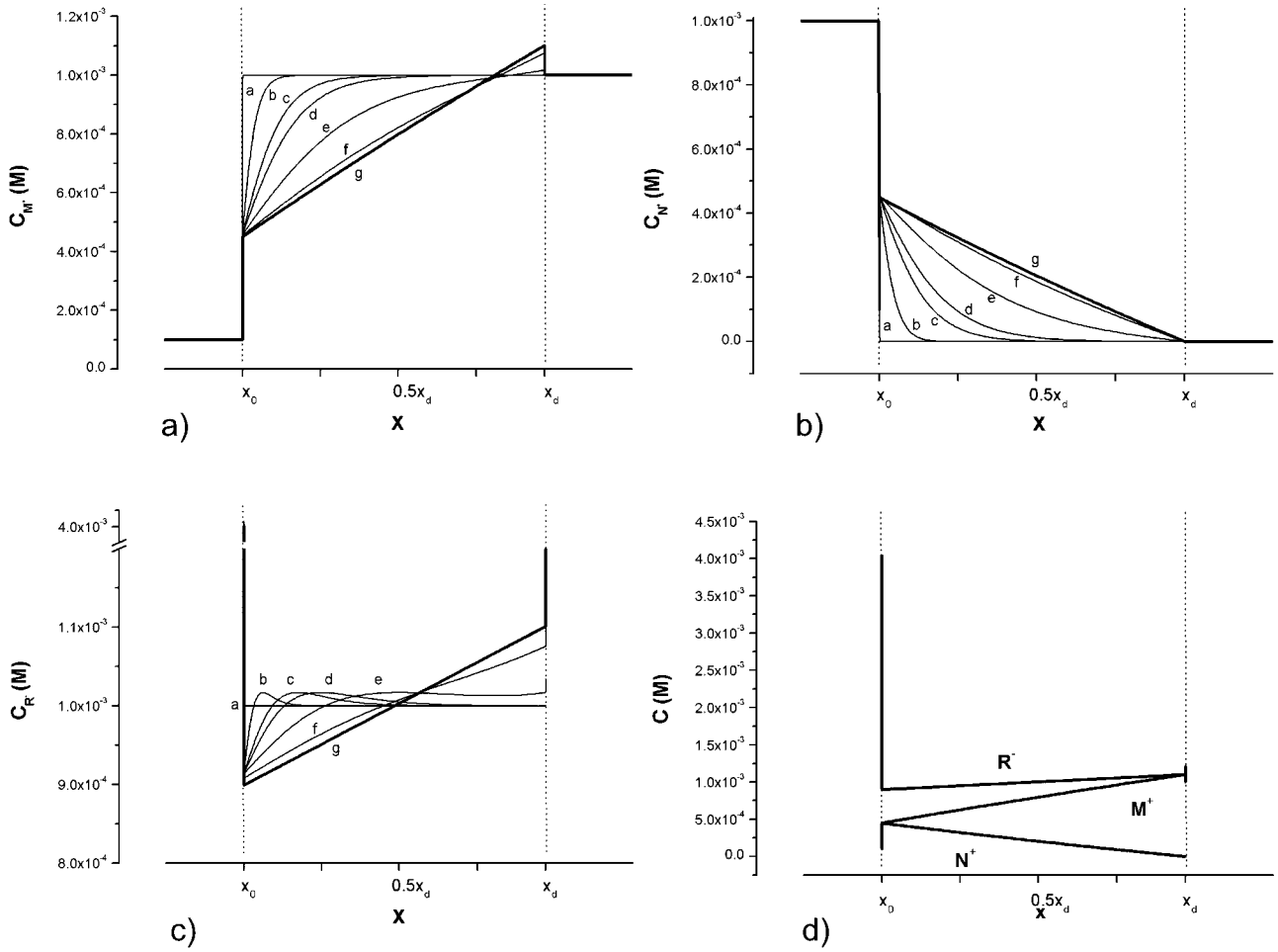

Figure 4. Case marked by (*) in Figure 3 ($[M^+] = 10^{-4}$, $D_M/D_N = 0.5$). Time-dependent concentration profiles: (a) M^+, (b) N^+, (c) R^-, and (d) steady state. Curves a−g in panels a−c show profiles after (a) 4×10^{-4}, (b) 1.64, (c) 13.1, (d) 26.2, (e) 104.8, (f) 420, and (g) 13 440 s (steady state).

due to manipulation of the transmembrane ion fluxes through plastic membranes,[58,76,83,84] which clearly support the necessity of including diffusion potential in interpretations of ISE response as was recently emphasized.[85−87]

Moreover, what was initially assumed was soon treated as proven fact, and in turn, as a starting point for further ad hoc modifications of the NE equation, forgetting that the NE equation is already an empirical postulate. Those modifications have been pursued by adding time dependence to the time-independent NE equation (by applying Fickian law for ions, assuming that they are uncharged, e.g., Morf et al.[88] or by guessing a time function, e.g., Hulanicki and Lewenstam[74]) or even by direct "improvements" of a mostly formal nature (by adding additional semiempirical parameter(s), e.g., Ren[89] or by postulating "more general" form(s) of the NP equation, e.g., Zhang et al.[90]). Ultimately, prejudicial claims concerning the potential formation process are made such as, "the transport through the membrane produces no electrical potential and definitely proves that the electrode potential is created via surface chemisorption charge".[91]

This manner of theorizing is characteristic of arbitrarily going too far (ad hocness), which should preferably be avoided.[92,93] To avoid ad hocness, either independent empirical tests of the assumptions or unbiased and sufficiently rich theoretical modeling is required. In the latter instance, i.e., the case of the electrodynamics of ionically conducting junctions and membranes discussed in this paper, modeling may—for instance—be performed by adopting the NPP equation system, which is general and rich enough in a physical sense to encompass the membrane problem. The NPP equation system allows calculation of the electrical potential difference between (bulks of) two solutions bathing the membrane and finding the electrical potential and concentration profiles as a function of space and time. Only then can drawing conclusions about time and space domains be justified.

TABLE 3: Time-Dependent Contributions from the Diffusion Potential to the Overall Potential for Different Diffusion Coefficient Ratios and Main Ion Concentrations[a]

D_M/D_N		0.1		0.5		2		10	
c_M	time	M	%M	M	%M	M	%M	M	%M
10^{-10}	$4 \cdot 10^{-4}$	13.92	22.4	2.09	3.9	−4.34	7.3	−8.15	12.5
	1.64	32.6	41.8	7.62	12.5	−10.83	14.8	−38.33	35.2
	13.1	32.73	41.8	7.68	12.6	−10.96	14.9	−40.45	36.3
	26.2	32.73	41.4	7.68	12.6	−10.98	14.9	−40.77	36.4
	104.8	31.67	38.8	7.7	12.5	−10.84	14.7	−38.81	34.3
	420	28.22	36.1	7.55	11.8	−10.2	13.4	−32.29	27.6
	13 440	26.85	35.8	7.36	11.5	−10	13.0	−31.40	26.6
10^{-4}	$4 \cdot 10^{-4}$	12.12	26.1	1.71	4.4	−3.13	7.3	−5.85	12.5
	1.64	23.99	42.5	4.29	10.1	−5.03	10.6	−11.14	19.9
	13.1	24.07	42.5	4.31	10.2	−5.05	10.6	−11.21	20.0
	26.2	24.07	42.0	4.32	10.2	−5.04	10.6	−11.21	20.0
	104.8	23.42	39.4	4.32	10.1	−4.98	10.5	−10.71	19.1
	420	21.35	37.1	4.28	9.7	−4.69	9.7	−9.01	15.9
	13 440	20.50	36.8	4.22	9.5	−4.57	9.4	−8.55	15.1

[a] Monovalent primary and interfering ions. M, diffusion potential (mV); M%, relative contribution of diffusion potential (%).

3.3.2. Simulated Calibration Curves. To estimate how many points were necessary for spatial discretization, the well-known, controversial case of a main divalent ion (M^{2+}) in the presence of a monovalent interfering ion (N^+) was considered. The ratio D_M/D_N was assumed to be equal to 1. Thus, with a sufficient number of points, the results obtained from the NPP model should be identical to earlier results obtained by Morf.[50] In the paper by Brumleve and Buck, space was divided into 71 "slices" (including 20 closely spaced points at each interface), which was considered sufficient for a good numerical description of the problem. This is true for the biionic case (M^+, N^+) presented there. However, the calibration curves of ISEs presented here are much more demanding, since one (inner reference) side of the membrane is bathed with a constant, relatively high concentration solution (10^{-3} M), while on the other (sample) side, the concentration ranges from 10^{-10} to 10^{-1} M. As seen from Figure 2, 71 points are not enough. The curves obtained for 501 and 1001 spatial points converge, and for this reason, 1001 points were used in all simulations.

In Figure 3, the steady state calibration curves for monovalent primary ion (M^+) in the presence of interfering ion (N^+) are shown. The sample solution (left side) contains a constant 10^{-3} M concentration of N^+ while the concentration of M^+ is varied from 10^{-1} to 10^{-10} M. The ratio of diffusion coefficients (D_M/D_N) is 0.1, 0.5, 1, 2, or 10. The rate constants for M^+, N^+, and R^- are $\vec{k}_M = \overleftarrow{k}_M = 10^{-1}$, $\vec{k}_N = 10^{-2}$, $\overleftarrow{k}_N = 10^{-1}$, $\vec{k}_R = \overleftarrow{k}_R = 0$, so $K_{M,N} = k_N/k_M = 0.1$ (see appendix C in the Supporting Information for details).

The diffusion coefficient ratios were chosen intentionally: the case $D_M/D_N = 0.1$ or 10 to compare with the classical biionic case, and the case $D_M/D_N = 0.5$ or 2 to give an example of what might be found in an actual ISE.[94]

The membrane was preconditioned in a solution of main ion (M^+/membrane(R^-)/M^+) so it contained 10^{-3} M M^+R^-. At time $t = 0$, the conditioning solution (M^+X^-) on the left side was replaced by one containing both M^+ and N^+ (M^+,N^+/membrane(R^-)/M^+).

Although the NPP model does not differentiate between boundary and diffusion potential, the terminology is retained in order to facilitate comparisons with conventional models. For this reason, the boundary potential is arbitrarily situated in space between the boundary and the 3.6×10^{-9} m within the membrane at both interfaces. The remaining part of the membrane interior is associated with the diffusion potential term. The pie charts above and below the top and bottom curves show the contributions to the overall potential from the boundary potential (white) and from the diffusion potential (black) at [M^+] = 10^{-10} and [M^+] = 10^{-4} M for $D_M/D_N = 0.1$ and 10, respectively.

As can be seen in Figure 3, the diffusion potential accounts for approximately 30% of the overall potential and cannot be ignored even at steady state. Before steady state is achieved, it also contributes significantly to the overall potential, as is shown in Table 3.

This case is analyzed in more detail by selecting one characteristic point on the calibration curve corresponding to equal contributions from the primary and interfering ions, marked by an asterisk in Figure 3. Time-dependent concentration profiles for M^+, N^+, and R^- are given in Figure 4a−c. The steady state concentration profiles for M^+, N^+, and R^- are given in Figure 4d. The concentration profiles obtained are—as a rule—nonlinear, even at steady state.

The time-dependent electrical potential profiles are given in Figure 5a. As can be seen, they are nonmonotonic and nonlinear.

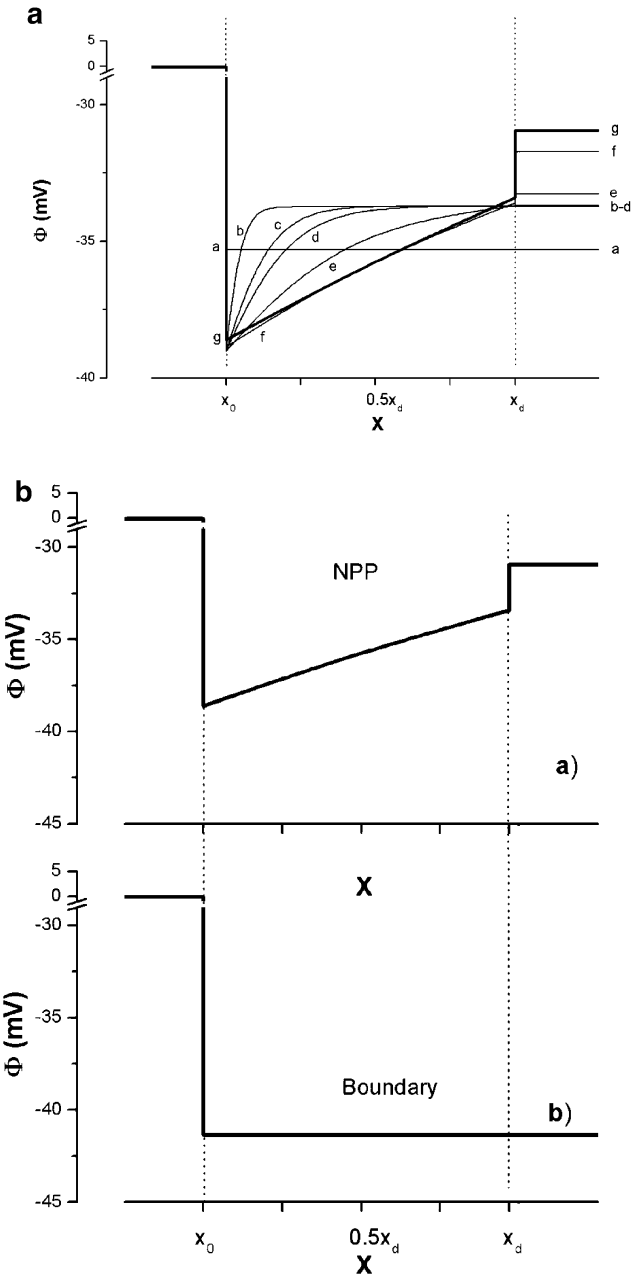

Figure 5. (a) Case marked by (*) in Figure 3 ([M^+] = 10^{-4}, $D_M/D_N = 0.5$). Time-dependent potential profiles. $\Phi(x,t) = \int_0^x E(x,t)\,dx$. Total membrane potential is $\Phi_{Tot}(x,t) = \int_0^d E(x,t)\,dx$. (b) Comparison of the (a) steady state NPP potential profile from panel a with that presumed by (b) boundary models.

A comparison of steady state potential profiles according to boundary and NPP models is shown in Figure 5b. According to the boundary model, the electrical potential drop is postulated to be located entirely at the left sample/membrane interface. The NPP model demonstrates a striking and documented difference. There are three uneven, but comparable, spatial contributions to the overall membrane potential, namely, the left sample/membrane boundary potential, the diffusion potential, and the right membrane/(inner) solution boundary potential.

The importance of this result should be emphasized because it contradicts many claims that the left sample/membrane boundary potential exclusively determines the ISE membrane potential, which is described by the NE equation. We in fact disclaim the general theoretical validity of the NE equation, although it can be valid in some special cases (i.e., at high

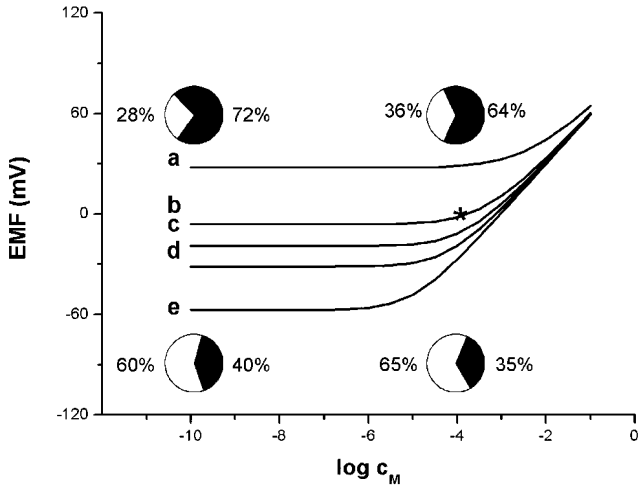

Figure 6. Calibration curves in the presence of primary ($[M^{2+}]$ = (10^{-10} to 10^{-1} M)) and interfering ($[N^{+}]$ = 0.15 M) ions calculated according to the NPP model: (a) $D_M = D_R = 1.0 \times 10^{-7}$, $D_N = 1.0 \times 10^{-6}$ cm^2/s ($D_M/D_N = 0.1$); (b) $D_M = D_R = 1.0 \times 10^{-7}$, $D_N = 2.0 \times 10^{-7}$ cm^2/s ($D_M/D_N = 0.5$); (c) $D_M = D_N = D_R = 1.0 \times 10^{-7}$ cm^2/s ($D_M/D_N = 1$); (d) $D_M = 2.0 \times 10^{-7}$, $D_N = D_R = 1.0 \times 10^{-7}$ cm^2/s ($D_M/D_N = 2$); (e) $D_M = 1.0 \times 10^{-6}$, $D_N = D_R = 1.0 \times 10^{-7}$ cm^2/s ($D_M/D_N = 10$), $k_M = k_M = 10^{-1}$, $k_N = 4.472 \times 10^{-4}$, $k_N = 10^{-1}$, $k_N/k_M = 4.472 \times 10^{-3}$. Pie charts express contributions of boundary potential (white) and inner membrane potential (black) for the outermost calibration curves (D_M/D_N = 0.1 or 10) at $[M^{+}] = 10^{-4}$ and $[M^{+}] = 10^{-10}$ M.

TABLE 4: Time-Dependent Contributions from the Diffusion Potential to the Overall Potential for Different Diffusion Coefficient Ratios and Main Ion Concentrations[a]

D_M/D_N		0.1		0.5		2		10	
c_M	time	M	%M	M	%M	M	%M	M	%M
10^{-10}	$4 \cdot 10^{-4}$	24.81	72.6	5.36	27.3	−4.64	19.8	−10.11	32.8
	1.64	29.87	77.0	7.34	32.5	−7.9	26.1	−26.35	47.8
	13.1	29.89	77.2	7.35	32.5	−7.93	26.1	−26.93	48.1
	26.2	29.88	77.8	7.35	32.5	−7.93	26.1	−27.02	48.2
	104.8	29.13	79.8	7.35	32.9	−7.88	25.8	−26.53	47.1
	420	26.97	75.2	7.26	34.4	−7.57	24.3	−23.81	41.7
	13 440	26.19	71.9	7.16	35.3	−7.42	23.6	−22.91	39.9
10^{-4}	4×10^{-4}	22.84	65.5	4.64	33.0	−3.6	22.0	−7.71	35.3
	1.64	26.95	67.4	5.89	38.4	−4.852	26.6	−11.22	42.2
	13.1	26.96	67.5	5.90	38.4	−4.86	26.6	−11.24	42.2
	26.2	26.95	68.0	5.90	38.5	−4.861	26.6	−11.25	42.2
	104.8	26.36	69.6	5.91	39.0	−4.825	26.3	−11.01	41.2
	420	24.74	66.4	5.86	41.2	−4.623	24.7	−9.94	37.0
	13 440	24.14	64.1	5.80	42.7	−4.52	23.9	−9.52	35.3

[a] Divalent primary ion and monovalent interfering ion. M, diffusion potential (mV); M%, relative contribution of diffusion potential (%).

concentration after infinite time). These cases may be found by inspecting time and concentration domains of the NPP model; see, e.g., Figure 3. In addition, the NPP model provides numerical verification for the semievident supposition that any difference in ion mobilities will give rise to diffusion potential.

To illustrate further the power of the NPP model, the results for the 2:1 charge ratio are shown. The calibration curves for the divalent primary ion (M^{2+}) in the presence of the monovalent interfering ion (N^{+}) are depicted in Figure 6. The sample solution (left side) contains a constant 0.15 M concentration of N^{+} while the concentration of M^{2+} is varied from 10^{-1} to 10^{-10} M.

The ratio of diffusion coefficients (D_M/D_N) is 0.1, 0.5, 1, 2, or 10. The rate constants for this new case were as follows: $\vec{k}_M = \overleftarrow{k}_M = 10^{-1}$, $\vec{k}_N = 4.472 \times 10^{-4}$ and $\overleftarrow{k}_N = 10^{-1}$, $\vec{k}_R = \overleftarrow{k}_R = 0$, and $K_{M,N} = 0.01$. The membrane was preconditioned in a

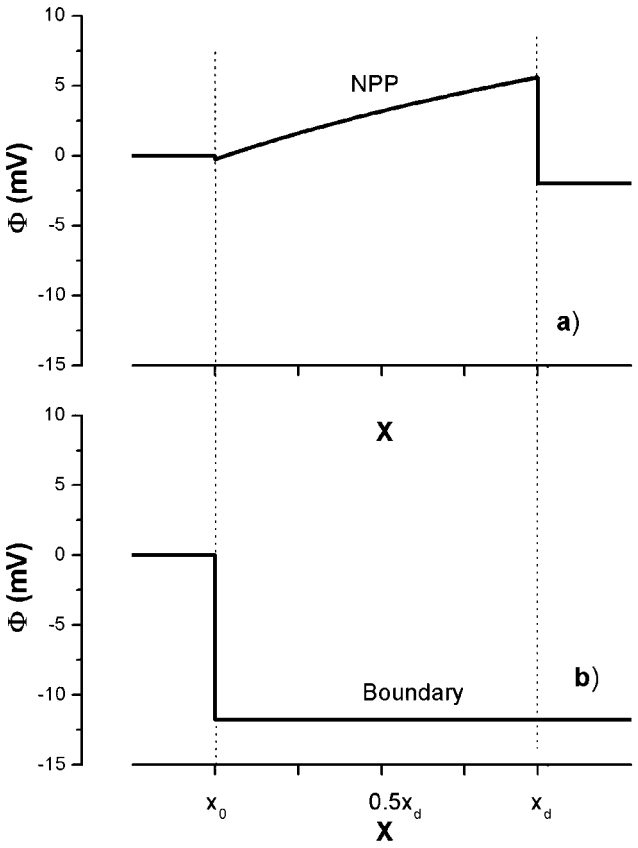

Figure 7. Comparison of the (a) steady state NPP potential profile with that presumed by (b) boundary models.

solution of main ion (M^{2+}/membrane(R^{-})/M^{2+}). At time $t = 0$, the conditioning solution on the left side was replaced by one containing both M^{2+} and N^{+} (M^{2+},N^{+}/membrane(R^{-})/M^{2+}). The values for all diffusion coefficient ratios are shown in Table 4.

Clearly, the diffusion potential contributions are even more significant in this case and certainly cannot be ignored. A comparison between the NPP and the boundary models (Figure 7) shows dramatic differences in the spatial potential distribution even under steady state.

In summary, we want to emphasize that the cases presented above are only representative examples. The NPP model can easily be extended to many other cases.

3.3.3. Benefits of the NPP Model. At first glance, it may seem that the NPP model is formally complicated whereas the boundary model is simple. Quite the opposite is in fact the case. Once the NPP code is written, one has a flexible and powerful tool that enables the inspection of numerous cases such as those discussed above. With the boundary model, different cases must be considered separately, and in each case, several—sometimes dubious—assumptions must be made. Then, after trivial but tedious algebra, one arrives at the final equation. Moreover, the final equation may not even necessarily be general. The illustration of such a case is shown in Figure 8.

The boundary model,[81] which allows for reasonably good results with a 2:1 charge ratio, results in a calibration curve exhibiting an extremum (dip) when extended to a 3:1 charge ratio, which is a signal of a theoretical anomaly. The latter cannot be seen in the curve generated from the same initial conditions by the NPP method. The boundary model dip is an artifact resulting from ad hoc assumptions. Even if its magnitude is small, its conceptual importance is unquestionable.

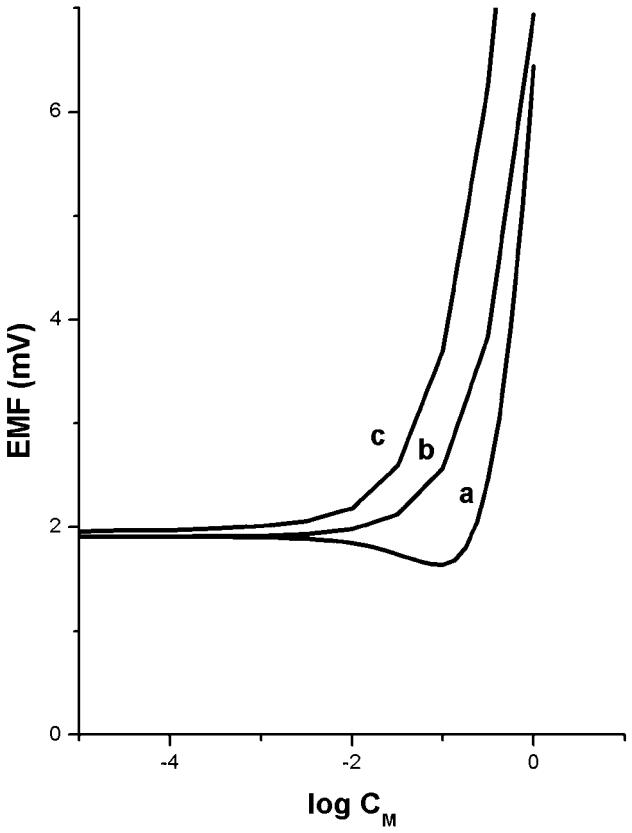

Figure 8. Calibration curves in the presence of primary ($[M^{3+}] = (10^{-5} - 10^{0}$ M)) and interfering ($[N^{+}] = 0.5$ M) ions calculated according to (a) phase boundary model, Bakker et al., eq 28,[81] $K_{M,N} = 10$; (b) NE eq 10, $K_{M,N} = 10$; (c) NPP model, $D_M = D_N = D_R = 1.0 \times 10^{-7}$ cm^2/s, $k_N = 3.107 \times 10^{-3}$, $k_N = k_M = k_M = 10^{-1}$cm/s ($k_N/k_M = 3.107 \times 10^{-2}$).

4. Conclusions

The application of the NPP method brings the modeling of liquid contact or membrane potential closer to physical relevance. For ISEs, the NPP model allows us to abandon the previously necessary split of membrane potential into boundary and diffusion potentials. It applies to ions of any charge. It gives access to both time and space domains. Consequently, analyses of transient membrane potential and its spatial distribution over the whole membrane are possible. In particular, it was demonstrated that both the interfaces and the membrane interior contribute to the overall membrane potential. This remains in sharp contrast with conventional ISE models, which locate the possible potential changes at the sample/membrane boundary.

The Planck and Henderson equations for liquid junctions and the NE equation for ISE membranes have been demonstrated to be special cases of the NPP model. The former gives the same result as the NPP model only at infinite time. Likewise, the NE description of ISE membranes matches that obtained from the NPP model only at high concentrations after infinite time.

This numerical method presented here is fully implicit. Finite difference discretization was used, and the resulting set of difference equations was solved via Newton−Raphson iteration. The implementation is written in the C++ programming environment. This makes the program's modifications (more dimensions, more advanced chemistry in the membrane, more advanced boundary conditions, variable dielectric permittivity, and diffusion coefficients) possible.

Acknowledgment. We thank Ari Ivaska for his support and interest in the course of this work. Financial support from the Finnish Academy via the Process Chemistry Group Centre of Excellence (PCG) is gratefully acknowledged. Financial support from the Graduate School in Chemical Engineering and partial financial support from the Polish Committee for Scientific Research via Grants KBN 3T09A-11118 and 7T08E-02520 are also acknowledged.

Supporting Information Available: Numerical model, electroneutrality paradox, and formulas for selectivity coefficients. This material is available free of charge via the Internet at http://pubs.acs.org.

References and Notes

(1) Lewenstam, A.; Zytkow, J. M. *Ion-Selective Electrodes*; Pergamon Press: New York, 1989; Vol. 5, pp 297−304.
(2) Zytkow, J. M.; Lewenstam, A. *Fresenius J. Anal. Chem.* **1990**, *338*, 225.
(3) IUPAC. *Pure Appl. Chem.* **1976**, *48*, 129.
(4) IUPAC. *Pure Appl. Chem.* **1994**, *66*, 2527.
(5) Cardenas, A. E.; Coalson, R. D.; Kurnikova, M. G. *Biophys. J.* **2000**, *79*, 80.
(6) Chen, D.; Lear, J.; Eisenberg, B. *Biophys. J.* **1997**, *72*, 97.
(7) Eisenberg, R. S. *J. Membr. Biol.* **1996**, *150*, 1.
(8) Eisenberg, R. S. *J. Membr. Biol.* **1999**, *171*, 1.
(9) Kurnikova, M. G.; Coalson, R. D.; Graf, P.; Nitzan, A. *Biophys. J.* **1999**, *76*, 642.
(10) Nonner, W.; Eisenberg, B. *Biophys. J.* **1998**, *75*, 1287.
(11) Lewenstam, A.; Zytkow, J. M. *Fresenius J. Anal. Chem.* **1987**, *326*, 308.
(12) Cohen, H.; Cooley, J. W. *Biophys. J.* **1965**, *5*, 145.
(13) Hafemann, D. R. *J. Phys. Chem.* **1965**, *69*, 4226.
(14) MacGillivray, A. D. *J. Chem. Phys.* **1967**, *48*, 2903.
(15) MacGillivray, A. D. *J. Chem. Phys.* **1969**, *52*, 3126.
(16) Brumleve, T. R.; Buck, R. P. *J. Electroanal. Chem.* **1978**, *90*, 1.
(17) Kontturi, A. K.; Kontturi, K.; Mafe, S.; Manzanares, J. A.; Niinikoski, P.; Vuoristo, M. *Langmuir* **1994**, *10*, 949.
(18) Kontturi, K.; Mafe, S.; Manzanares, J. A.; Pellicer, J. *J. Electroanal. Chem.* **1994**, *378*, 111.
(19) Kontturi, K.; Manzanares, J. A.; Murtomaki, L.; Schiffrin, D. J. *J. Phys. Chem. B* **1997**, *101*, 10801.
(20) Mafe, S.; Pellicer, J.; Aguilella, V. M. *J. Phys. Chem.* **1986**, *90*, 6045.
(21) Mafe, S.; Pellicer, J.; Aguilella, V. M. *An. Fis., Ser. B* **1987**, *83*, 96.
(22) Manzanares, J. A.; Mafe, S.; Pellicer, J. *J. Phys. Chem.* **1991**, *95*, 5620.
(23) Manzanares, J. A.; Murphy, W. D.; Mafe, S.; Reiss, H. *J. Phys. Chem.* **1993**, *97*, 8524.
(24) Rudolph, M. *J. Electroanal. Chem* **1994**, *375*, 89.
(25) Samson, E.; Marchand, J. *J. Colloid Interface Sci.* **1999**, *215*, 1.
(26) Moya, A. A.; Horno, J. *J. Phys. Chem. B* **1999**, *103*, 10791.
(27) Langtangen, H. P. *Computational Partial Differential Equations. Numerical Methods and Diffpack Programming*; Springer-Verlag: Berlin, 1999.
(28) Sokalski, T.; Lewenstam, A. *Electrochem. Commun.* **2001**, *3*, 107.
(29) MacInnes, D. A. *The Principles of Electrochemistry*; Dover: New York, 1961.
(30) Chan, A. D. C.; Li, X.; Harrison, D. J. *Anal. Chem.* **1992**, *64*, 2512.
(31) Li, Z.; Rothmaier, M.; Harrison, D. J. *Anal. Chem.* **1996**, *68*, 1726.
(32) Zwickl, T.; Schneider, B.; Lindner, E.; Sokalski, T.; Schaller, U.; Pretsch, E. *Anal. Sci.* **1998**, *14*, 57.
(33) Nernst, W. *Z. Phys. Chem.* **1888**, *2*, 613.
(34) Nernst, W. *Z. Phys. Chem.* **1889**, *4*, 129.
(35) Planck, M. *Ann. Phys. Chem.* **1890**, *39*, 161.
(36) Planck, M. *Ann. Phys. Chem.* **1890**, *40*, 561.
(37) Buck, R. P. *J. Membr. Sci.* **1984**, *17*, 1.
(38) Dole, M. *J. Am. Chem. Soc.* **1931**, *53*, 4260.
(39) Donnan, F. G. *Z. Elektrochem.* **1911**, *17*, 572.
(40) Henderson, P. *Z. Phys. Chem.* **1907**, *59*, 118.
(41) Henderson, P. *Z. Phys. Chem.* **1908**, 325.
(42) Nikolskii, B. P. *Acta Physicochem. USSR* **1937**, *7*, 597.
(43) Schlögl, R. *Z. Phys. Chem. (Frankfurt am Main)* **1954**, 305.
(44) Teorell, T. *Trans. Farday Soc.* **1937**, *33*, 1053.
(45) Johnson, K. R. *Ann. Phys. (Leipzig)* **1904**, *14*, 995.
(46) Pleijel, H. *Z. Phys. Chem.* **1910**, *72*, 1.
(47) Eisenman, G. *Glass Electrodes for Hydrogen and Other Cations*; M. Dekker: New York, 1967; p 192.

(48) Helfferich, F. *Ion Exchange*; McGraw-Hill: New York, 1962.
(49) Lakshminarayanaiah, N. *Membrane Electrodes*; Academic Press: New York, 1976.
(50) Morf, W. E. *The Principles of Ion-Selective Electrodes and of Membrane Transport*; Akademiai Kiado: Budapest, 1981.
(51) Janata, J. *Principles of Chemical Sensors*; Plenum Press: New York, 1989.
(52) Aguilella, V. M.; Mafe, S.; Pellicer, J. *Electrochim. Acta* **1987**, *32*, 483.
(53) Feldberg, S. W. *Electrochem. Commun.* **2000**, *2*, 453.
(54) Morf, W. E. *Anal. Chem.* **1977**, *49*, 810.
(55) Lewenstam, A. *Anal. Proc. (London)* **1991**, *28*, 106.
(56) Lewenstam, A.; Maj-Zurawska, M.; Hulanicki, A. *Electroanalysis* **1991**, *3*, 727.
(57) Lewenstam, A. *Scand. J. Clin. Lab. Invest., Suppl.* **1994**, *54*, 11.
(58) Sokalski, T.; Maj-Zurawska, M.; Hulanicki, A.; Lewenstam, A. *Electroanalysis* **1999**, *11*, 632.
(59) Haber, F.; Klemensiewicz, Z. *Z. Phys. Chem.* **1909**, *67*, 385.
(60) Guggenheim, E. A. *J. Phys. Chem.* **1929**, *33*, 842.
(61) Guggenheim, E. A. *J. Phys. Chem.* **1930**, *34*, 1540.
(62) Stefanova, O. K. Shultz. M. M.; Materova, E. A.; Nikolskii, B. P. *Viest. Leningr. University* **1963**, *4*, 93.
(63) Shultz, M. M.; Stefanova, O. K. *Viest. Leningr. University* **1967**, *6*, 103.
(64) Conti, F.; Eisenman, G. *Biophys. J.* **1965**, *5*, 247.
(65) Conti, F.; Eisenman, G. *Biophys. J.* **1965**, *5*, 511.
(66) Sandblom, J. P. E. G. W. J. L. *J. Phys. Chem.* **1967**, *71*, 3862.
(67) Goldman, D. E. *J. Gen. Physiol.* **1943**, *27*, 37.
(68) Hodgkin, A. L.; Katz, B. *J. Physiol.* **1949**, *108*, 37.
(69) Sollner, K. *Z. Elektrochem.* **1930**, *36*, 36.
(70) Meyer, K. H.; Sievers, J. F. *Helv. Chim. Acta* **1936**, *19*, 655.
(71) Meyer, K. H.; Sievers, J. F. *Trans. Farday Soc.* **1937**, *33*, 1073.
(72) Wuhrmann, H.-R.; Morf, W. E.; Simon, W. *Helv. Chim. Acta* **1973**, *56*, 1011.
(73) Buck, R. P.; Sandifer, J. R. *J. Phys. Chem.* **1973**, *77*, 2122.
(74) Hulanicki, A.; Lewenstam, A. *Anal. Chem.* **1981**, *53*, 1401.
(75) Bakker, E.; Nagele, M.; Schaller, U.; Pretsch, E. *Electroanalysis* **1995**, *7*, 817.
(76) Sokalski, T.; Ceresa, A.; Zwickl, T.; Pretsch, E. *J. Am. Chem. Soc.* **1997**, *119*, 11347.
(77) Morf, W. E.; Badertscher, M.; Zwickl, T.; de Rooij, N. F.; Pretsch, E. *J. Phys. Chem. B* **1999**, *103*, 11346.
(78) Bakker, E.; Meruva, R. K.; Pretsch, E.; Meyerhoff, M. E. *Anal. Chem.* **1994**, *66*, 3013.
(79) Mi, Y.; Bakker, E. *Anal. Chem.* **1999**, *71*, 5279.
(80) Schaller, U.; Bakker, E.; Spichiger, U. E.; Pretsch, E. *Anal. Chem.* **1994**, *66*, 391.
(81) Bakker, E.; Buehlmann, P.; Pretsch, E. *Chem. Rev.* **1997**, *97*, 3083.
(82) Buhlmann, P.; Amemiya, S.; Yajima, S.; Umezawa, Y. *Anal. Chem.* **1998**, *70*, 4291.
(83) Sokalski, T.; Zwickl, T.; Bakker, E.; Pretsch, E. *Anal. Chem.* **1999**, *71*, 1204.
(84) Sokalski, T.; Ceresa, A.; Fibbioli, M.; Zwickl, T.; Bakker, E.; Pretsch, E. *Anal. Chem.* **1999**, *71*, 1210.
(85) Mikhelson, K. N.; Lewenstam, A. *Sens. Actuators, B* **1998**, *48*, 344.
(86) Mikhelson, K. N.; Lewenstam, A.; Didina, S. E. *Electroanalysis* **1999**, *11*, 793.
(87) Mikhelson, K. N.; Lewenstam, A. *Anal. Chem.* **2000**, *72*, 4965.
(88) Morf, W. E.; Badertscher, M.; Zwickl, T.; Reichmuth, P. ; de Rooij, N.F.; Pretsch, E. *J. Phys. Chem. B* **2000**, *104*, 8201.
(89) Ren, K. *Talanta* **2000**, *52*, 1157.
(90) Zhang, W.; Fakler, A.; Demuth, C.; Spichiger, U. E. *Anal. Chim. Acta* **2000**, *375*, 211.
(91) Pungor, E. *Talanta* **1997**, *34*, 1505.
(92) Popper, K. R. *Conjectures and Refutations*; Routledge and Kegan Paul: London, 1972.
(93) Popper, K. R. *Objective Knowledge*; Clarendon Press: Oxford, 1974.
(94) Armstrong, R. D.; Covington, A. K.; Evans, G. P. *Anal. Chim. Acta* **1984**, *166*, 103.